

Tests results of ENDF/B.VIII.1.β2 in GND format

CSEWG 2023

Marie-Anne Descalle, Gregory Patel, Caleb Mattoon,
Godfree Gert, Bret Beck

November 16, 2023

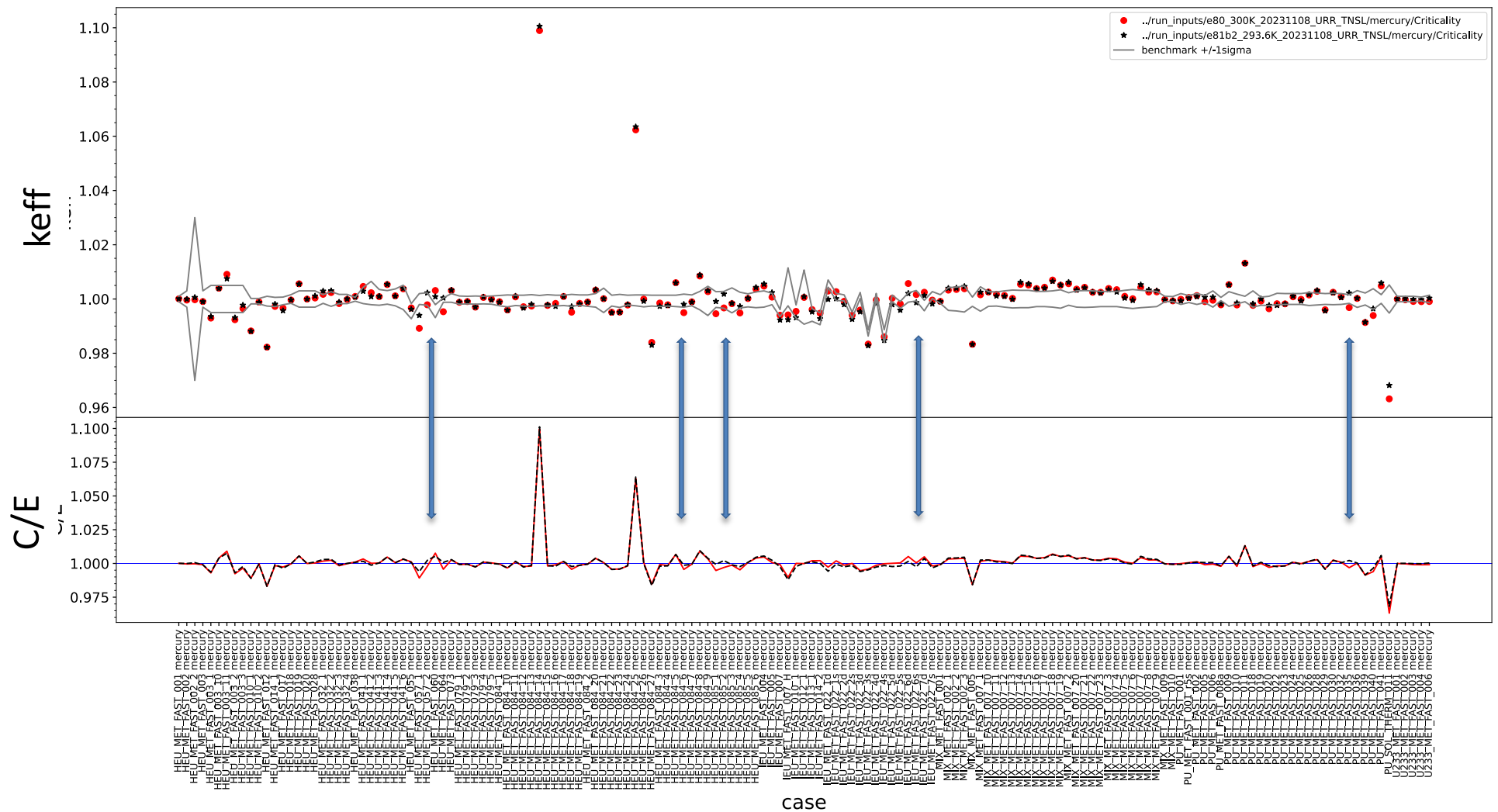


The ENDF/B-VIII.x evaluations were processed with FUDGE 6.1.0 in GNDS 2.0 format

- Beta 2: 557 isotopes
- URR Probability Tables except for
 - ENDF/B-VIII.0 timeout: 17; fail: Sn112, Pt192 T=300.0K
 - ENDF/B-VIII.1.beta1, long processing time Pa231, Pa 233, Eu; no fail T=293.6K
 - ENDF/B-VIII.1.beta2 T=293.6K
- TNSL processed, 25/88 TNSL files accessed by Mercury,
 - cases with H2O,D2O,CH2, Be, BeO
- Metis: 147 Fast Critical Assemblies/ 73 Thermal
- Mercury MC transport code
 - Version: 5.36.1
 - GIDI+: 3.27.9

Criticality: comparison to ENDF/B-VIII.0

$C_{e81beta2}$ and C_{e80}



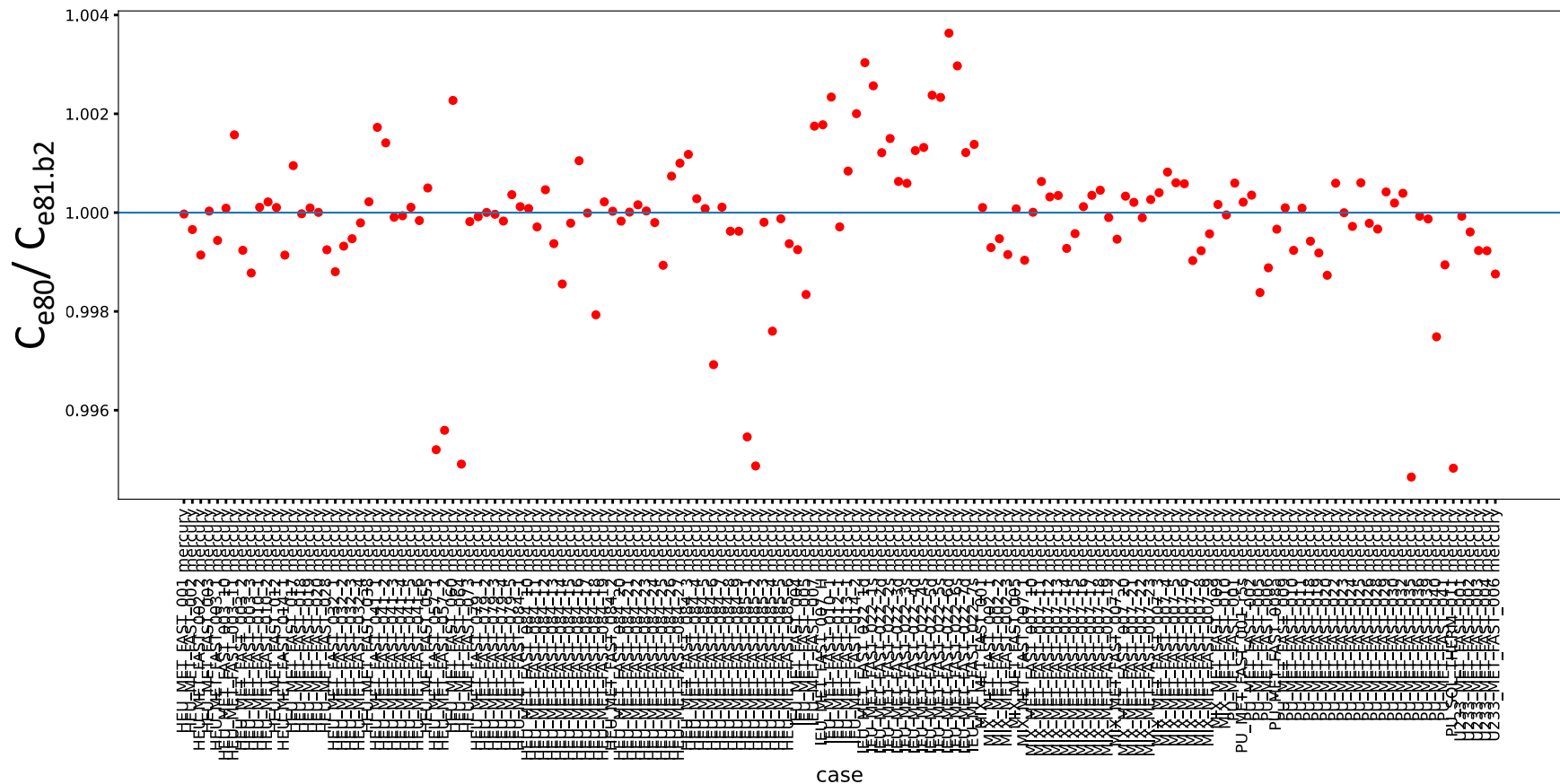
Criticality: comparison to ENDF/B-VIII.0

$$C_{e80}/C_{e81.beta2}$$

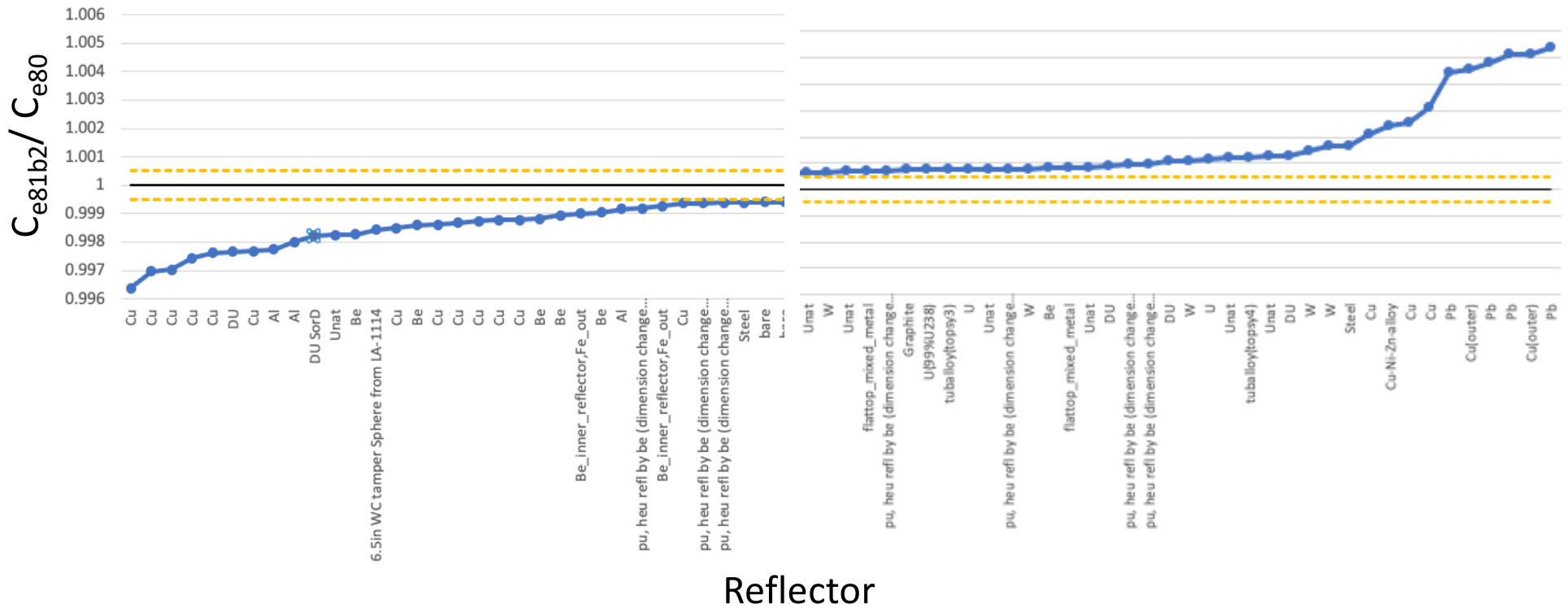
Criticality

keff(test1) / keff(test2) results

test1 = ../run_inputs/e80_300K_20231108_URR_TNSL/mercury/Criticality
test2 = ../run_inputs/e81b2_293.6K_20231108_URR_TNSL/mercury/Criticality

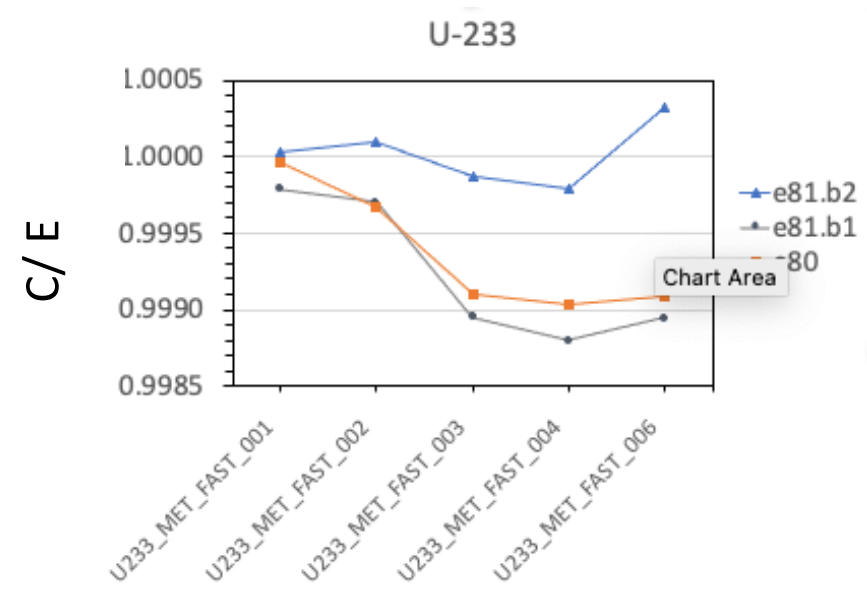
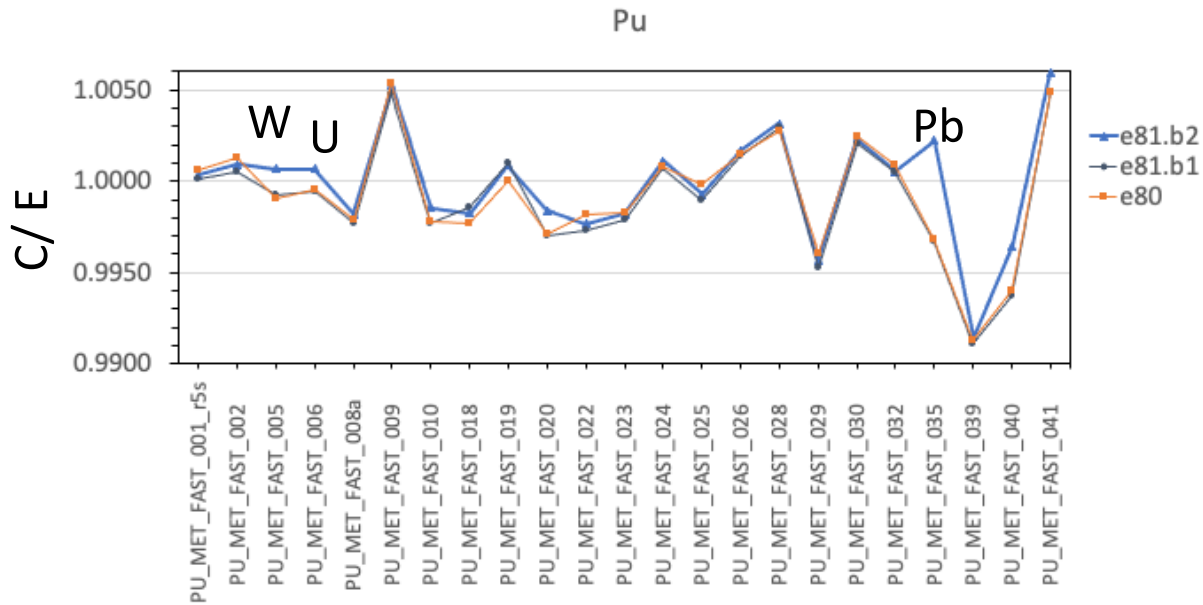


Now, Criticality: C_{e81b2}/C_{e80}



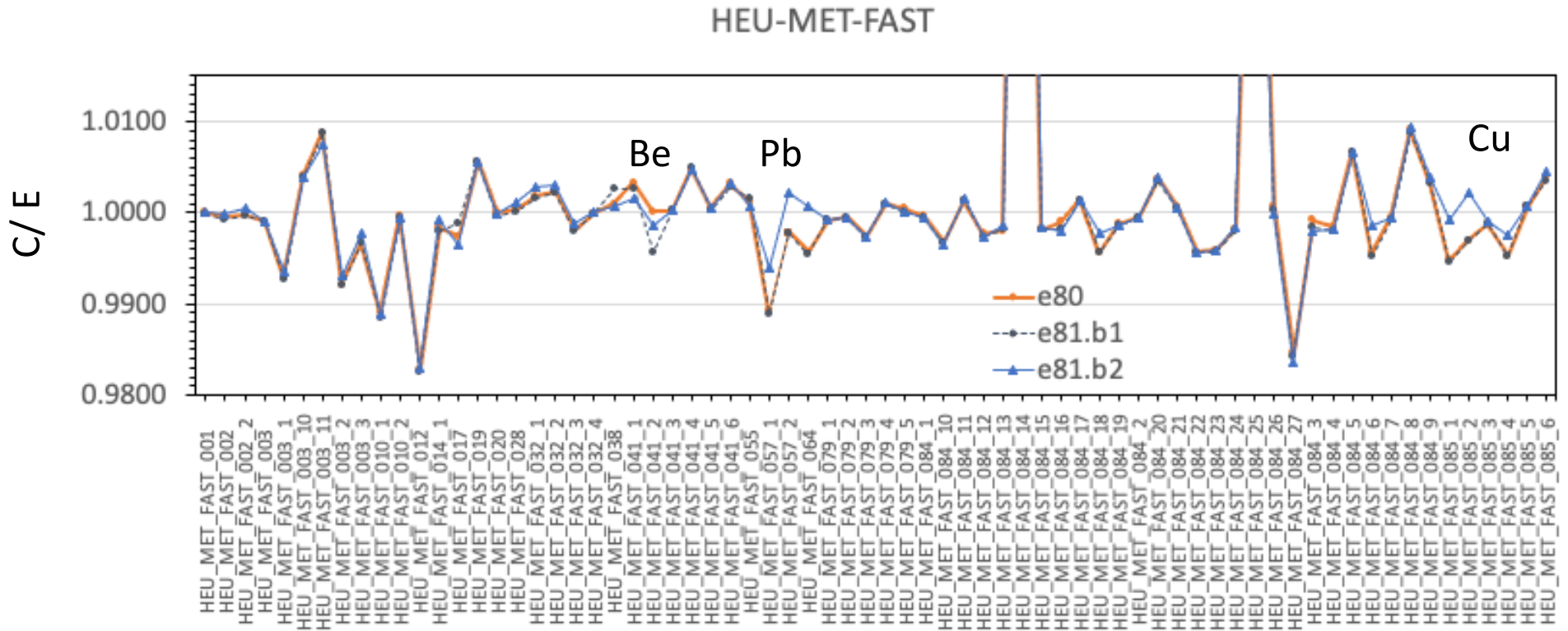
Cases with IMF22(Cu) reflectors and Pb show largest differences; Al, Du and U nat & W

C/E Criticality: PU, U233



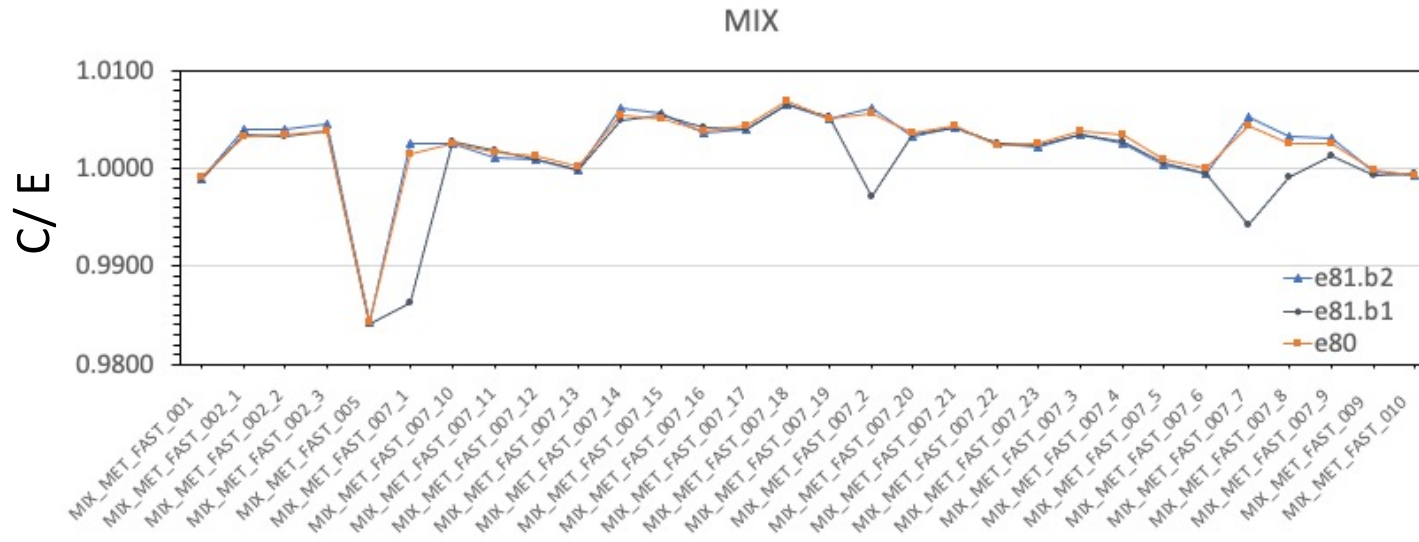
Jezebel rev 5 simplified excellent agreement, PMF good agreement
UMF overall improvement

C/E Criticality: PU, HEU, U233



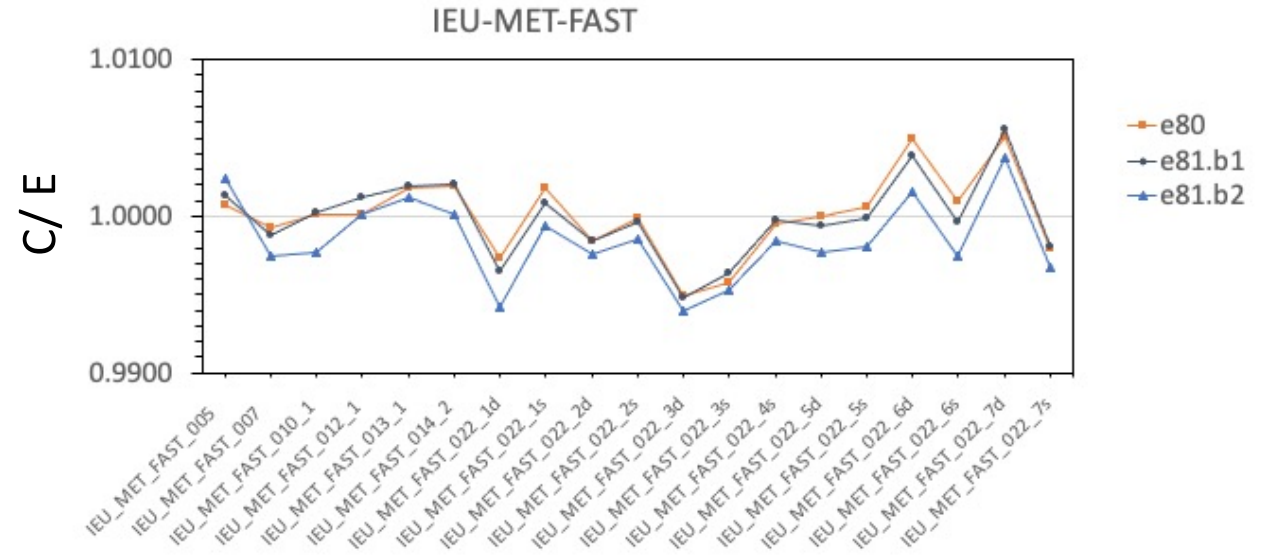
HMF improvements seem to be driven by changes to Cu, Pb, Be

C/E Criticality: MIX, IEU

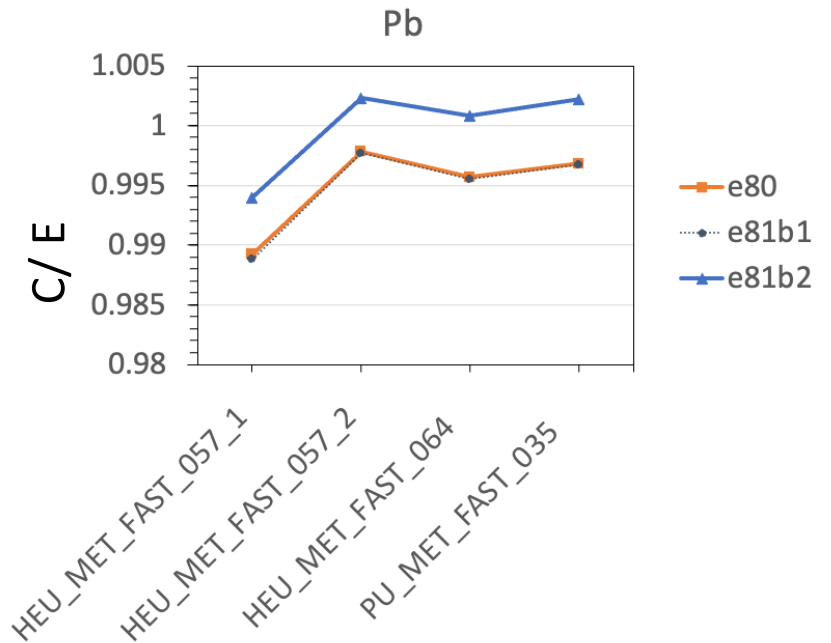
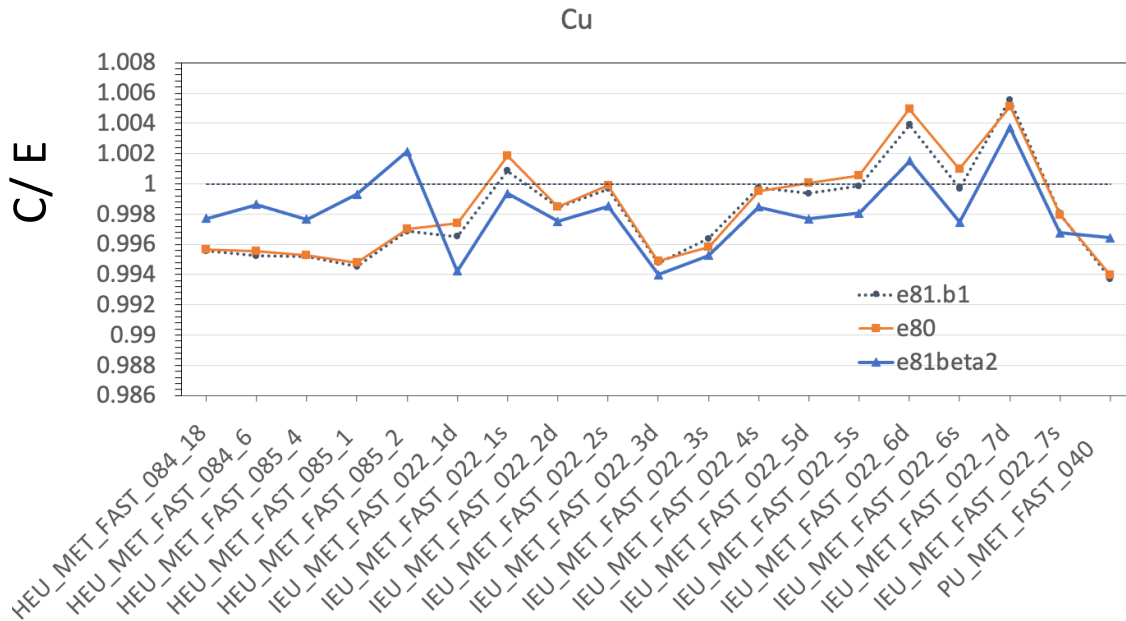


E81.b1 low k_{eff} :Be

IMF overall decrease in k_{eff} , overall poorer agreement when including IMF022 (Cu)

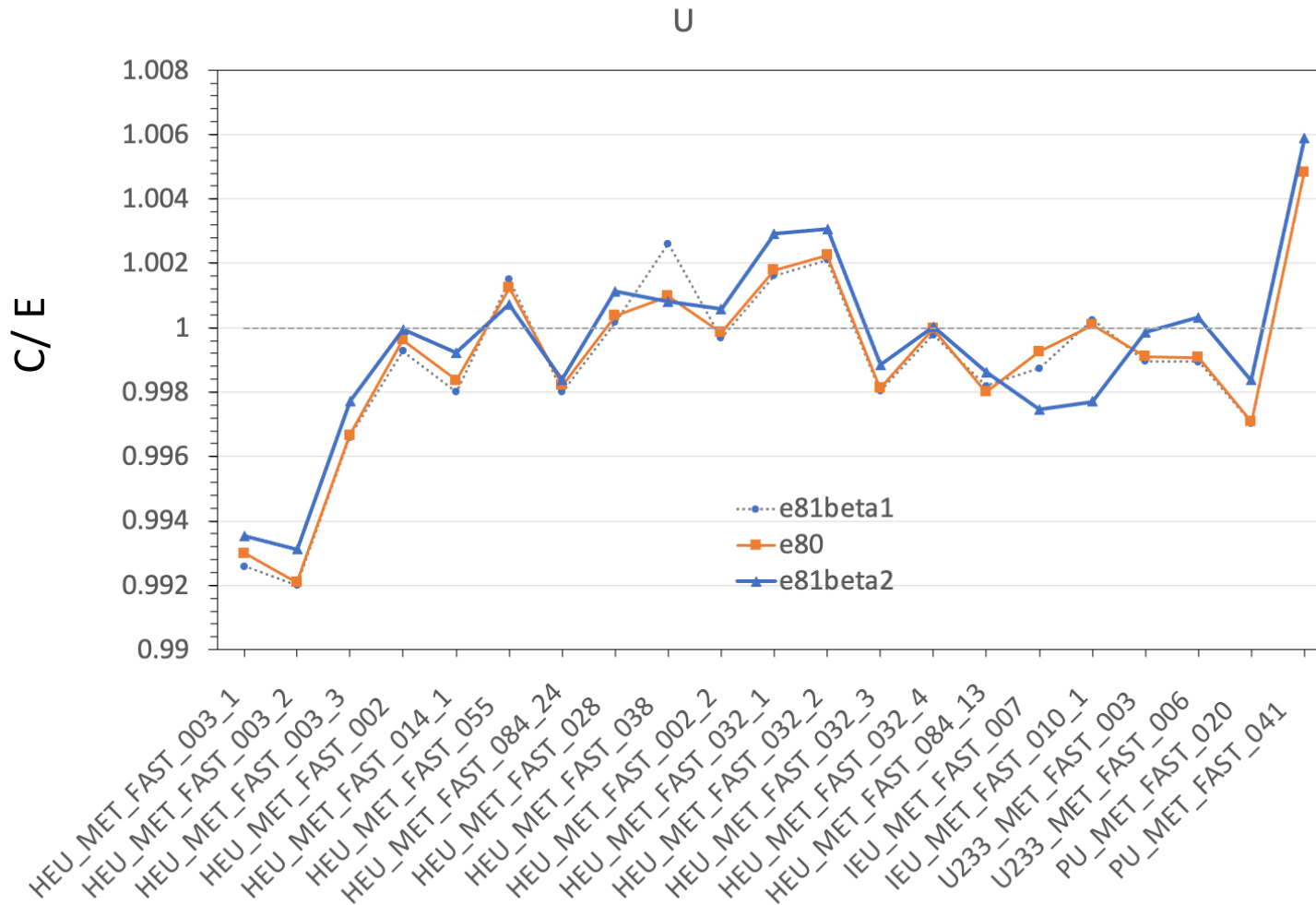


Reflector: Cu, Pb

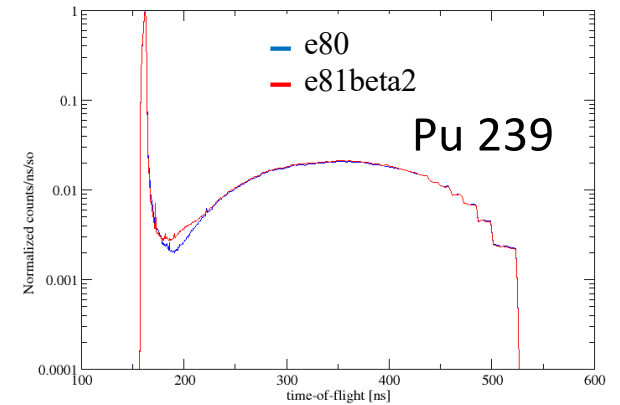
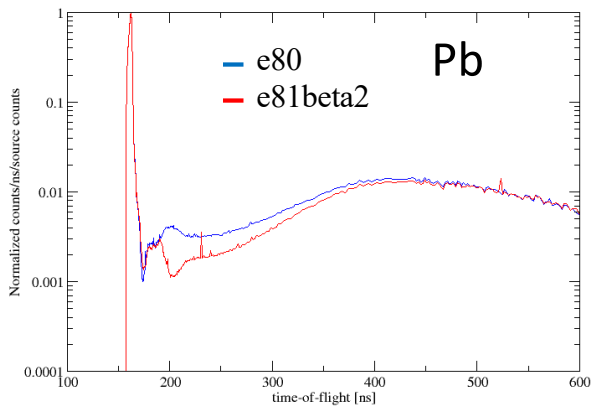
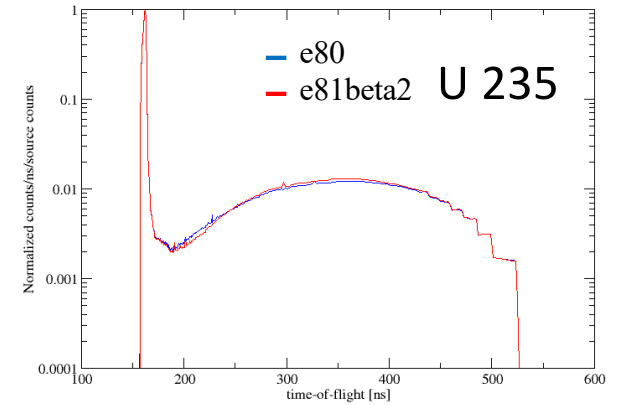
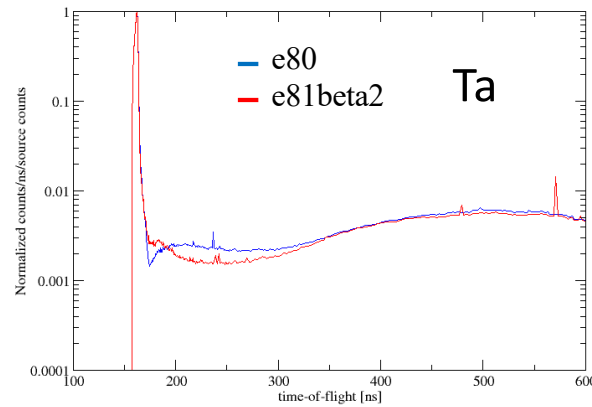
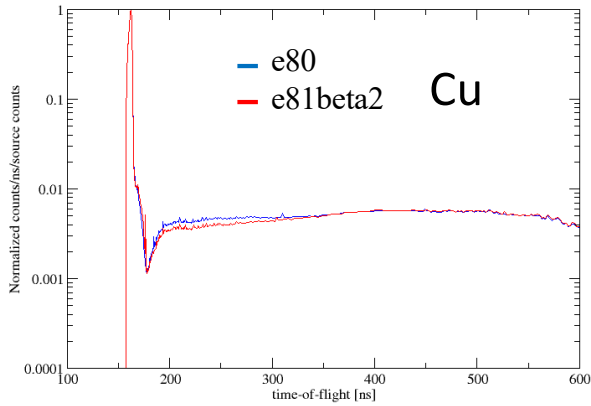


Cu: HMF better agreement while for IMF agreement is worse
 Pb: C/E improved

Reflector: U, DU, tuballoy

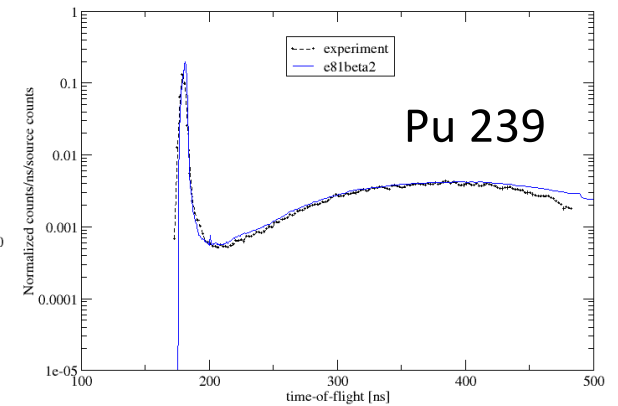
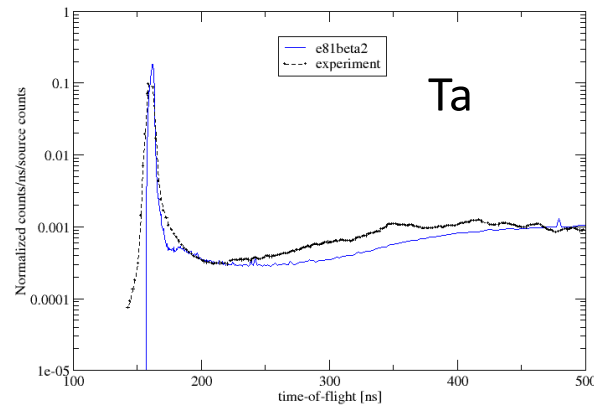
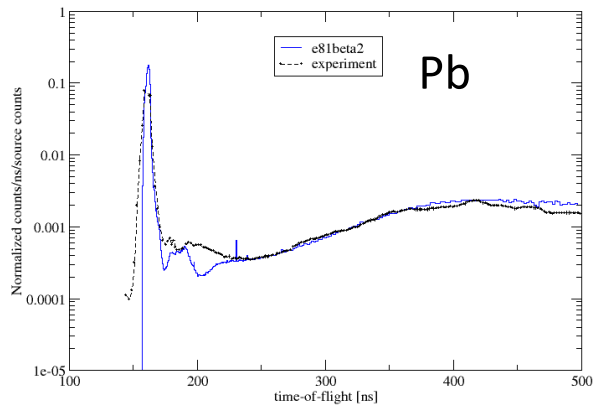
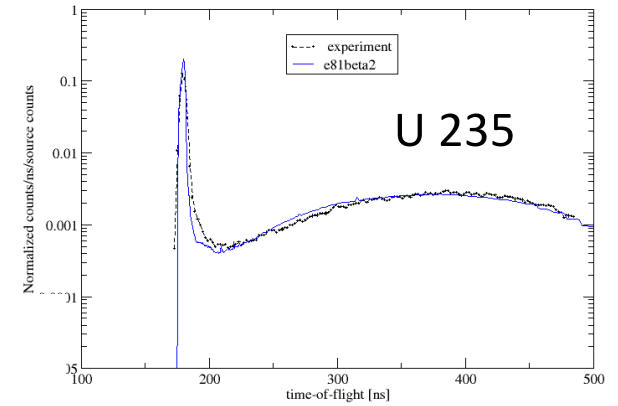
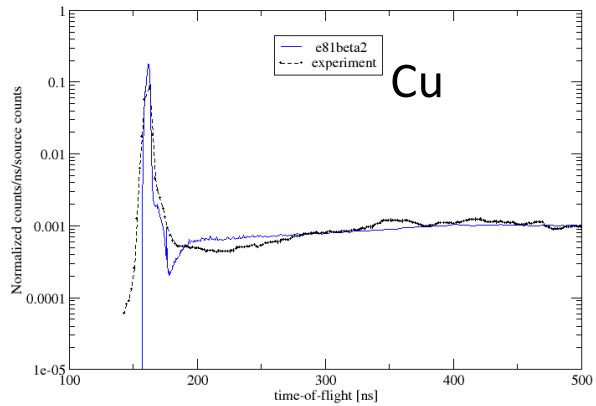


LLNL pulsed spheres



Pb, Ta, Pu239 show spectral changes, smaller effect seen for Cu and U235

LLNL pulsed spheres



Pu239 improved; U235 and Cu similar; Ta local improvement; Pb should be reviewed

Fission Ratios: comparison to e80

- Mercury/GNDS – MCNP6.2/ACE * Brown et al. NDS 148 (2018)
- Reaction rates are normalized by $^{235}\text{U}(n,f)$

Benchmark	Reaction Ratio	$^{238}\text{U}(n,f)$	$^{237}\text{Np}(n,f)$	$^{233}\text{U}(n,f)$	$^{239}\text{Pu}(n,f)$
Godiva	Mercury e81b2	0.1580	0.8301	1.5795	1.3831
	Mercury e80	0.1583	0.8315	1.5796	1.3846
	MCNP e80 *	0.1583	0.8318	1.5793	1.3846
	Mercury e81b2/e80	0.9980	0.9983	0.9999	0.9989
Jezebel	Mercury e81b2	0.2108	0.9711	1.5661	1.4246
	Mercury e80	0.2107	0.9768	1.5661	1.4271
	MCNP e80 *	0.2121	0.9770	1.5660	1.4273
	Mercury e81b2/e80	1.0005	0.9942	1.0000	0.9982
Flatop25	Mercury e81b2	0.1448	0.7726	1.5779	1.3607
	Mercury e80	0.1451	0.7732	1.5779	1.3621
	MCNP e80 *	0.1451	0.7735	1.5664	1.3622
	Mercury e81b2/e80	0.9979	0.9992	1.0000	0.9990

Fission Ratios: C_{e81b2}/E

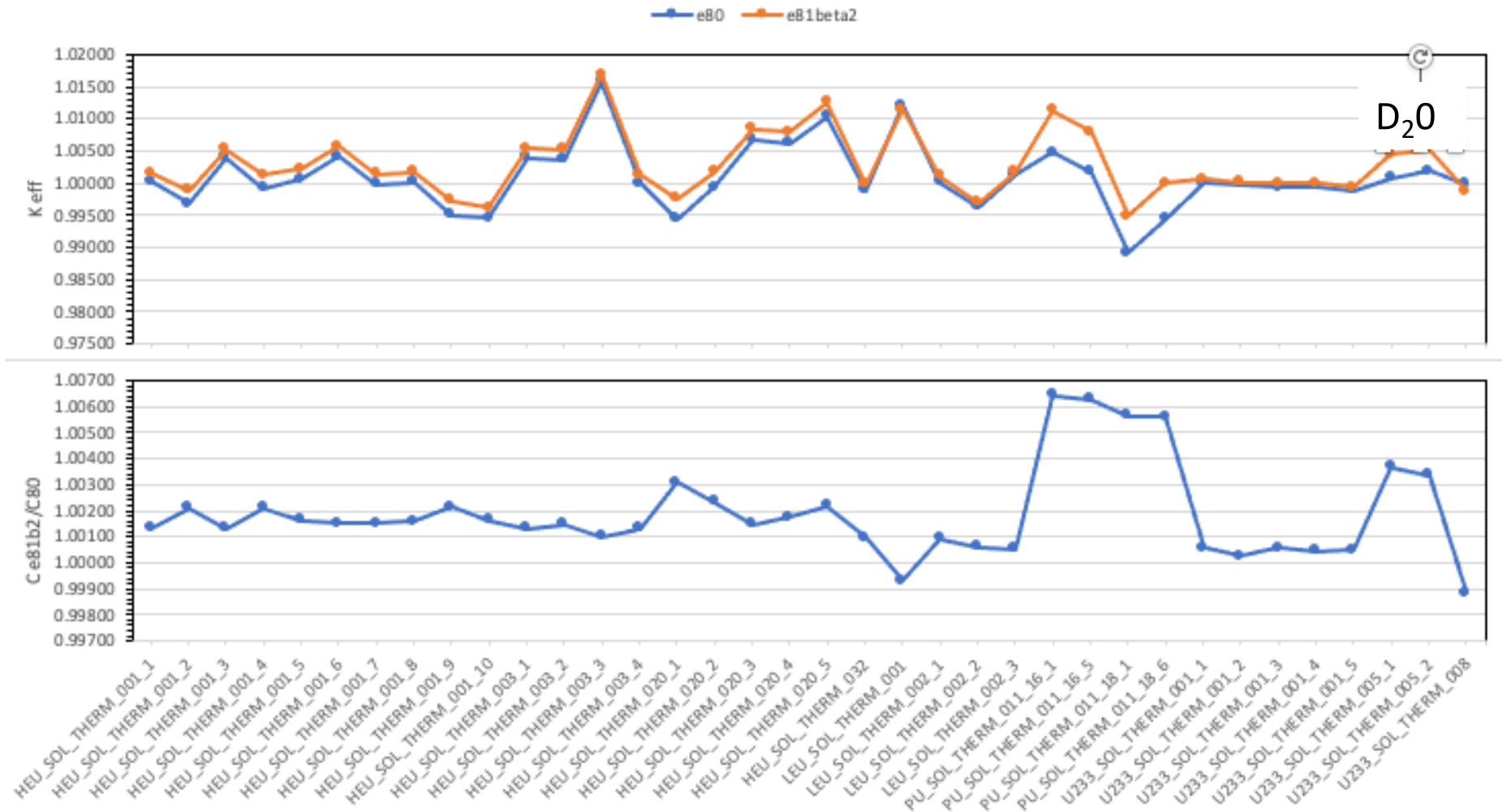
Assembly	Quantity	U238f/U235f	Np237f/U235f	U233f/U235f	Pu239f/U235f
Godiva (HMF001)	Calc	0.1580	0.8301	1.5795	1.3831
	Exp-B	0.1643±0.0018	0.8516±0.012	*	1.4152±0.014
	Exp-A	0.1642±0.0018	0.8370±0.013	1.5900±0.03	1.4020±0.025
	Calc/Exp	0.9614	0.9748	0.9934	0.9773
Jezebel (PMF001)	Calc	0.2108	0.9711	1.5661	1.4246
	Exp-B	0.2133±0.0023	0.9835±0.014	*	1.4609±0.013
	Exp-A	0.2137±0.0023	0.9620±0.016	1.578±0.027	1.448±0.029
	Calc/Exp	0.9883	0.9874	0.9925	0.9752
Jezebel-23 (UMF001)	Calc	0.2114	0.9851		
	Exp-B	0.2131±0.0026	0.997±0.015		
	Exp-A	0.2131±0.0023	0.977±0.016		
	Calc/Exp	0.9922	0.9881		
Flatop-25 (HMF028)	Calc	0.1448	0.7726	1.5779	1.3607
	Exp-B	0.1492±0.0016	0.7804±0.01	1.608±0.003	1.3847±0.012
	Exp-A	0.1490±0.002	0.7600±0.01	1.600±0.003	1.3700±0.02
	Calc/Exp	0.9705	0.9900	0.9813	0.9827
Flatop-Pu (PMF006)	Calc	0.1778	0.8503		
	Exp-B	0.1799±0.002	0.8561±0.012		
	Exp-A	0.1800±0.003	0.84±0.01		
	Calc/Exp	0.9881	0.9933		
Flatop-23 (UMF006)	Calc	0.1873	0.8994		
	Exp-B	0.1916±0.0021	0.9103±0.013		
	Exp-A	0.1910±0.003	0.8900±0.01		
	Calc/Exp	0.9776	0.9880		

Summary

- C/E of U233-MET-FAST benchmarks were improved when using ENDF/B-VIII.1 beta2 compared to VIII.0 and VIII.1beta1
- C/E of HEU and PU-MET-FAST did not show major changes using ENDF/B-VIII.1 beta2
- C/E of IEU-MET-FAST benchmarks are lower and worse than those simulated with VIII.0 and VIII.1beta1
- Changes seen were driven by reflector, mostly Pb, Cu and Be
 - Be ENDF/B-VIII.1 beta2 results are improved compared to ENDF/B-VIII.1 beta1
 - Cu ENDF/B-VIII.1 beta2 results are improved for HEU-MET-FAST cases, not for IEU-MET-FAST but unlikely to be related to the Cu evaluations
 - Pb ENDF/B-VIII.1 beta2 results are improved for 4 cases, the Pulsed sphere spectrum shows odd features.

Backup

Thermal assemblies



Then: Beta 1 Fission Ratios

- Mercury/GNDS – MCNP6.2/ACE * Brown et al. NDS 148 (2018)
- Reaction rates are normalized by $^{235}\text{U}(n,f)$

Benchmark	Reaction Ratio	$^{238}\text{U}(n,f)$	$^{237}\text{Np}(n,f)$	$^{233}\text{U}(n,f)$	$^{239}\text{Pu}(n,f)$
Godiva	Mercury e81b1	0.1580	0.8301	1.5795	1.3830
	Mercury e80	0.1583	0.8315	1.5796	1.3846
	MCNP e80 *	0.1583	0.8318	1.5793	1.3846
	Mercury e81b1/e80	0.9981	0.9983	0.9999	0.9988
Jezebel	Mercury e81b1	0.2110	0.9719	1.5662	1.4246
	Mercury e80	0.2107	0.9768	1.5661	1.4271
	MCNP e80 *	0.2121	0.9770	1.5660	1.4273
	Mercury e81b1/e80	1.0013	0.9949	1.0001	0.9982
Flatop25	Mercury e81b1	0.1447	0.7728	1.5779	1.3608
	Mercury e80	0.1451	0.7732	1.5779	1.3621
	MCNP e80 *	0.1451	0.7735	1.5664	1.3622
	Mercury e81b1/e80	0.9972	0.9995	1.0000	0.9990

TNSL files available to Mercury

- <alias id="1401" pid="HinC5O2H8"/>
- <alias id="1501" pid="HinYH2"/>
- <alias id="1701" pid="HinZrH"/>
- <alias id="1801" pid="HinH2O"/> 6 std 32tnsl ///cog 231/190
- <alias id="1901" pid="HinCH2"/> 5 tns1 80/190
- <alias id="1902" pid="DinD2O"/> 5 tns1
- <alias id="4809" pid="Be-metal"/> 56
- <alias id="4909" pid="BeinBeO"/> 2
- <alias id="6512" pid="benzene"/>
- <alias id="6712" pid="CinSiC"/>
- <alias id="6612" pid="reactor-graphite-30P"/>
- <alias id="6812" pid="reactor-graphite-10P"/>
- <alias id="6912" pid="crystalline-graphite"/>
- <alias id="7914" pid="NinUN"/>
- <alias id="8716" pid="OinD2O"/>
- <alias id="8816" pid="OinUO2"/>
- <alias id="8916" pid="OinBeO"/>
- <alias id="13927" pid="tnsl-Al27"/>
- <alias id="26956" pid="tnsl-Fe56"/>
- <alias id="14728" pid="SiinSiC"/>
- <alias id="14928" pid="SiO2-alpha"/>
- <alias id="39989" pid="YinYH2"/>
- <alias id="40900" pid="ZrinZrH"/>
- <alias id="92838" pid="UinUN"/>
- <alias id="92938" pid="UinUO2"/>



Disclaimer

This document was prepared as an account of work sponsored by an agency of the United States government. Neither the United States government nor Lawrence Livermore National Security, LLC, nor any of their employees makes any warranty, expressed or implied, or assumes any legal liability or responsibility for the accuracy, completeness, or usefulness of any information, apparatus, product, or process disclosed, or represents that its use would not infringe privately owned rights. Reference herein to any specific commercial product, process, or service by trade name, trademark, manufacturer, or otherwise does not necessarily constitute or imply its endorsement, recommendation, or favoring by the United States government or Lawrence Livermore National Security, LLC. The views and opinions of authors expressed herein do not necessarily state or reflect those of the United States government or Lawrence Livermore National Security, LLC, and shall not be used for advertising or product endorsement purposes.

This work was performed under the auspices of the U.S. Department of Energy by Lawrence Livermore National Laboratory under contract DE-AC52-07NA27344. Lawrence Livermore National Security, LLC